High-spin levels in ^{191}Pt and ^{193}Pt and the triaxial rotor model*

S. K. Saha, M. Piiparinen,† J. C. Cunnane,‡ and P. J. Daly
Chemistry Department, Purdue University, West Lafayette, Indiana 47907

C. L. Dors, T. L. Khoo, and F. M. Bernthal
Departments of Chemistry and Physics and Cyclotron Laboratory, Michigan State University, East Lansing, Michigan 48824

(Received 27 August 1976)

The high-spin level structures of the transitional nuclei ^{191}Pt and ^{193}Pt have been studied by $(\alpha,3n\gamma)$ reactions on enriched Os targets. The measurements included γ-ray singles, comprehensive γ-γ coincidences, half-life determinations, and γ-ray angular distributions. The extensive ^{191}Pt and ^{193}Pt level schemes established are reported here. In both nuclei, decoupled $\nu i_{13/2}{}^{-1}$ bands, strongly resembling the ground bands of the adjacent core nuclei, and many other high-spin positive parity states have been located. Low-lying $21/2^-$ bands have also been observed in both nuclei and they are described as semidecoupled bands with microscopic structures dominated by three-quasiparticle components of the type $(\nu i_{13/2}{}^{-2},\nu j^{-1})$. The abundant information about $\nu i_{13/2}$ level families obtained in these experiments and in a complementary ^{191}Au decay study is discussed, and it is shown that these complex level spectra can be accounted for rather well in terms of the coupling of an $i_{13/2}$ neutron hole to a triaxially deformed core.

[NUCLEAR REACTIONS ^{190}Os, ^{192}Os$(\alpha,3n\gamma)$, $E=31$–46 MeV; measured E_γ, $I_\gamma(\theta)$, γ-γ coin, $T_{1/2}$; ^{191,193}Pt deduced level schemes, J, π.]

I. INTRODUCTION

Recently there has been a sharp revival of interest in the asymmetric rotor description of shape transitional nuclei. Of particular significance has been the work of Meyer ter Vehn,[1] who showed that the complex unique parity level spectra of odd-A nuclei observed in the $A=135$ and $A=190$ mass regions can be closely reproduced using a model of a high-j particle (or hole) coupled to a rotating triaxial core. Toki and Faessler[2] have extended the model to include the known softness of the core by a generalized variable moment of inertia (VMI) treatment.

We have investigated[3] the high-spin level structures of the transitional nuclei $^{186-194}$Pt by $(\alpha,xn\gamma)$ in-beam spectroscopy. In the odd-A nuclei, strongly populated $\nu i_{13/2}$ decoupled bands, resembling the ground bands of the adjacent core nuclei, were observed. Several additional strong deexcitation cascades connecting other high-spin $(\geq\frac{11}{2})$ positive parity members of the $\nu i_{13/2}$ family were also identified. In a complementary study[4] of the electron capture decay of 3.1-h ^{191}Au, low-spin $\nu i_{13/2}$ levels in ^{191}Pt were located and characterized. We have already reported briefly[5] on the rather complete $\nu i_{13/2}$ level family established by the combined studies, and have shown that the model of an $i_{13/2}$ hole coupled to a triaxial core ($\gamma\sim 30^\circ$) is impressively successful in accounting for the experimental findings.

Here we present and discuss the detailed results of the in-beam γ-ray investigations of the ^{191}Pt and ^{193}Pt level structures.

II. EXPERIMENTAL PROCEDURE

The ^{191}Pt and ^{193}Pt level schemes were investigated by $(\alpha,3n\gamma)$ reactions on isotopically enriched targets of ^{190}Os (95%) and ^{192}Os (98%), using α-particle beams from the Michigan State University cyclotron. Since the instruments and experimental techniques employed were similar to those described in our earlier article[6] on the ^{190}Pt and ^{192}Pt level structures, only a summary of the procedures and some samples of the data obtained are given here.

Singles γ-ray spectra were measured with Ge(Li) spectrometers at seven different α-particle bombarding energies spanning the range 31–46 MeV, and the γ rays of ^{191}Pt and ^{193}Pt were identified from their excitation functions. A typical γ-ray spectrum recorded is shown in Fig. 1. For both reactions, γ-ray angular distributions with respect to the beam direction were measured at five angles in the range 90°–140°, and values of the A_2/A_0 and A_4/A_0 coefficients were extracted for all well-resolved γ rays of moderate to strong intensity. Comprehensive three-parameter (γ,γ,t) coincidence measurements were performed using two Ge(Li) detectors, and prompt coincidence spectra gated on approximately 80 different γ rays in each nucleus studied were obtained. Some important ^{193}Pt coincidence spectra are shown in Fig. 2.

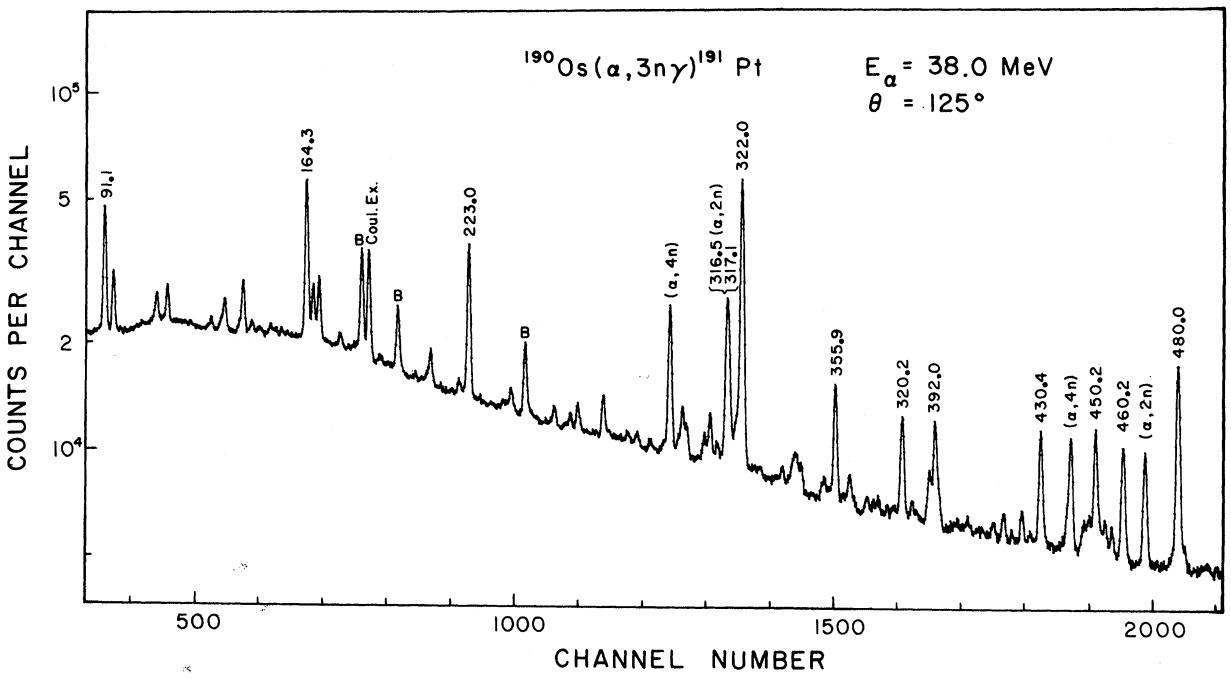

FIG. 1. A portion of a typical γ-ray singles spectrum. The peaks labeled B arise from background radiations of known origin.

Short-lifetime determinations were performed with a planar Ge(Li) spectrometer by recording a prompt γ-ray spectrum and nine delayed spectra spanning the ~50-ns time interval between cyclotron beam bursts. In Fig. 3, some of the data which established the existence of a 3.1± 0.5 ns isomer in ^{193}Pt are shown. Similar measurements for the ^{190}Os$(\alpha, 3n)$ reaction revealed an analogous isomer with $T_{1/2} = 1.5 \pm 0.4$ ns in ^{191}Pt. The only ^{191}Pt and ^{193}Pt radiations observed to decay with half-lives longer than these were the γ rays known to occur in the deexcitation of the low-lying 95-μs and 4.3-d $\frac{13}{2}^+$ isomeric states.[7]

III. RESULTS

The energies and relative intensities of the γ rays assigned to ^{191}Pt and ^{193}Pt are listed in Tables I and II together with the angular distribution coefficients and inferred transition multipolarities. The level schemes shown in Figs. 4 and 5 were constructed on the basis of the comprehensive γ-γ coincidence data, the transition intensities, and the detailed excitation function results. The delayed γ-ray spectra recorded during the nanosecond lifetime measurements provided strong support for the accuracy of these schemes.

Inspection of Figs. 4 and 5 reveals a close and detailed resemblance between the high-spin level spectra of ^{191}Pt and ^{193}Pt. The strongly populated $\frac{13}{2}^+$, $\frac{17}{2}^+$, $\frac{21}{2}^+$,... level sequences constitute favored decoupled $\nu i_{13/2}$ bands, which have level spacings very similar to those of the ground bands in the adjacent core nuclei ^{192}Pt and ^{194}Pt. Less commonly observed and of more particular interest here are the many additional positive parity levels at moderate excitation energies, which must also be members of the unique parity $\nu i_{13/2}$ level families. In each nucleus, these additional levels include a particularly low-lying $\frac{11}{2}^+$, two $\frac{15}{2}^+$ levels some 300–400 keV higher in energy, and one $\frac{17}{2}^+$ and two (or three) $\frac{19}{2}^+$ levels in the 600–1200 keV energy range. Structural relationships between some of these levels are strongly suggested by their electromagnetic deexcitation properties. For example, the lower energy $\frac{15}{2}^+$ level in each nucleus deexcites predominantly to the $\frac{11}{2}^+$ level, whereas the other $\frac{15}{2}^+$ level deexcites almost exclusively to the $\frac{13}{2}^+$ "bandhead." The observed branching patterns indicate that the $\frac{11}{2}^+$ and lowest $\frac{15}{2}^+$ and $\frac{19}{2}^+$ levels in ^{191}Pt and ^{193}Pt are of similar character. In Ref. 5, these levels were classified as members of unfavored decoupled bands, corresponding to incomplete alignment with a j projection of approximately $\frac{11}{2}$ on the core angular momentum R, and it was pointed out that the occurrence of such bands at very low energies in Pt nuclei is a consequence of the triaxial shape of the

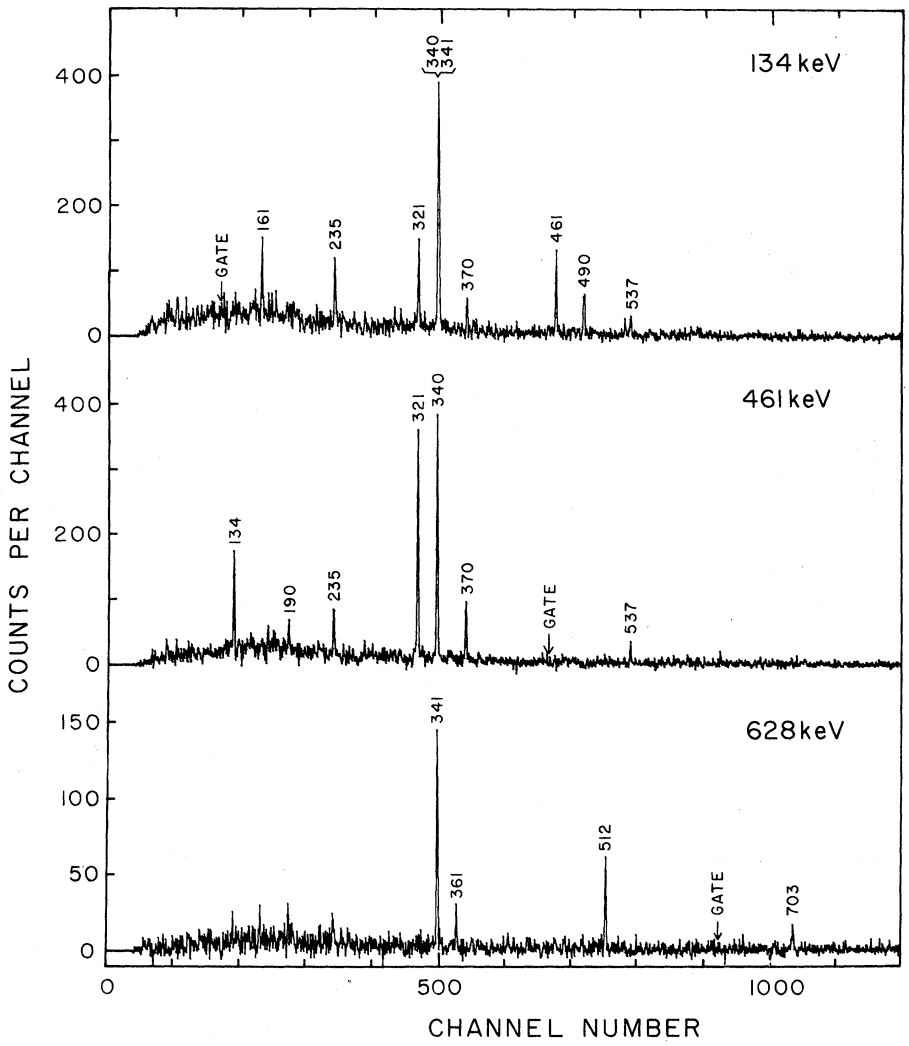

FIG. 2. Some important γ-γ coincidence spectra observed in the ^{193}Pt study.

core and of the location of the Fermi surface inside the $i_{13/2}$ shell.

Our knowledge of the $\nu i_{13/2}$ levels in ^{191}Pt is now unusually detailed, with information about low-spin family members from our ^{191}Au decay study,[4] and about high-spin members from the present work. In the case of ^{193}Pt, the levels reported here are the only positive parity levels known. Immediate prospects for learning about the low-spin $\nu i_{13/2}$ members in ^{193}Pt seem unpromising since it appears[8] that only negative parity levels are populated following the EC decay of ^{193}Au, which has a much smaller decay energy than ^{191}Au. In the following section the $\nu i_{13/2}$ level families in ^{191}Pt and ^{193}Pt will be discussed further.

In each nucleus, the sequence of negative parity levels starting with $\frac{21}{2}^-$ is also populated rather strongly. As has been noted previously,[3,9,10] such $\frac{21}{2}^-$ bands occur systematically in odd-A Pt and Hg nuclei. They appear to be closely related to the 5^- bands observed at similar excitation energies in the neighboring even-A nuclei, which have been interpreted[3,9-11] as semidecoupled bands with intrinsic structures dominated by two-quasiparticle components of the type $(\nu i_{13/2}^{-1}, \nu j^{-1})$. This description can be extended to the odd-A nuclei, where the $\frac{21}{2}^-$, $\frac{25}{2}^-$, ... level sequences may be attributed to the coupling of the 5^-, 7^-, ... core states with an additional $\nu i_{13/2}$ hole.[3,9,10] The marked structural resemblances between the $\frac{21}{2}^-$ bands in ^{191}Pt and ^{193}Pt and the 5^- bands in ^{192}Pt and ^{194}Pt strongly favor such an interpretation. Even more telling support is provided by the $\frac{25}{2}^- \rightarrow \frac{21}{2}^-$ $B(E2)$ values extracted from the measured

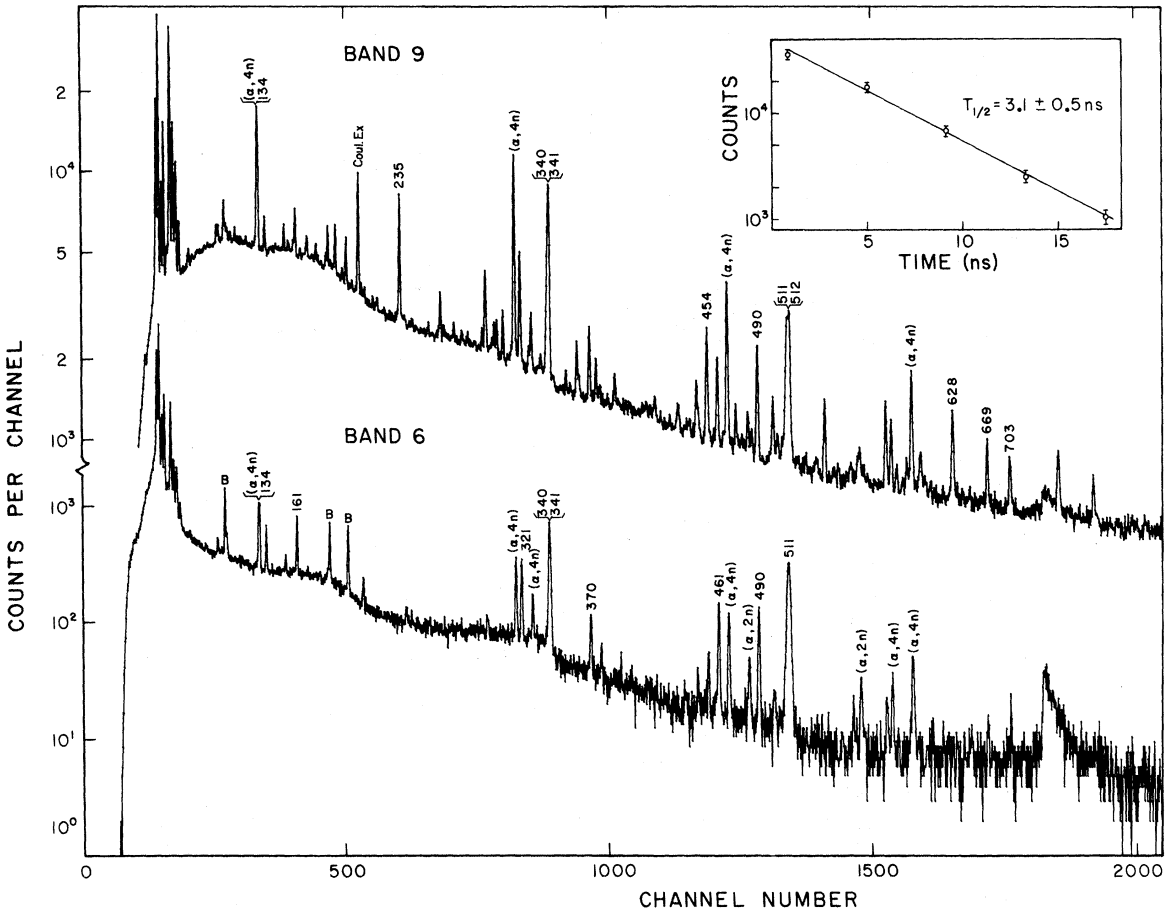

FIG. 3. The prompt (upper) and one of several delayed (lower) ^{193}Pt spectra recorded in the lifetime determination, and (inset) the half-life data obtained.

lifetimes, which are within a factor of 1.5 of the known $7^- \rightarrow 5^-$ $B(E2)$ values in ^{192}Pt and ^{194}Pt.

IV. MODEL CALCULATIONS

We have calculated[5] the energies and branching intensities of the low-lying positive parity levels in ^{191}Pt and ^{193}Pt using a model of a $\nu i_{13/2}$ hole coupled to a triaxial rotor, following closely the treatment developed by Meyer ter Vehn.[1] It is emphasized that the values of the parameters entering these calculations were not adjusted to fit the odd-A spectral data but were derived by the standard procedures proposed in Ref. 1. Specifically, the deformation and asymmetry parameters β and γ were obtained from the energies of the 2_1^+, 4_1^+, and 2_2^+ levels in the adjacent even-A Pt nuclei and the position of the Fermi level was estimated, for each nucleus, and for the appropriate γ, by inspecting the single particle level scheme of Larsson.[12] The initial calculations using these parameters reproduced the main features of the ^{191}Pt and ^{193}Pt level spectra surprisingly well. Somewhat better agreement with the data was obtained by introducing modified pairing factors of the form $(u_1u_2+v_1v_2)$,[5] an *ad hoc* procedure adopted from Ref. 13, which has the effect of reducing the Coriolis matrix elements connecting states on opposite sides of the Fermi surface. Such reductions have previously been found necessary for fitting $i_{13/2}$ band structures in axially symmetric rare earth nuclei.

Earlier[5] we have presented a comparison between the experimental and calculated level energies and branching ratios for the extensive $\nu i_{13/2}$ level family in ^{191}Pt. Although the overall agreement between theory and experiment provided persuasive evidence for triaxial shapes in Pt nuclei, two rather serious discrepancies were noted. Firstly, the calculated energies were generally too high, with particularly large deviations from experiment for the highest spin states. This has

TABLE I. Transitions in ^{191}Pt observed in the reaction ^{190}Os(α, 3n) with 37.0 MeV α particles. Estimated uncertainties in the least significant figures are shown in parentheses.

γ-ray energy (keV)	Relative intensity at 125°	Angular distribution A_2/A_0	A_4/A_0	Inferred multipolarity	Placement (keV)
48.2(3)	a			$M2$	149 → 101
91.1(1)	292(20)			$E2$	101 → 10
144.3(3)	12(2)	0.18(14)			
151.1(5)	8(2)				
164.3(1)	312(22)	0.25(7)	−0.16(7)	$E2$	1546 → 1381
168.8(1)	85(9)	0.00(16)	−0.09(17)		1471 → 1303
207.8(6)	20(6)				1158 → 951
209.2(2)	39(5)	−0.25(7)	−0.06(8)	$E1$ or $M1$	1591 → 1381
223.0(1)	287(20)	−0.21(7)	0.02(7)	($E1$)	1381 → 1158
259.8(3)	15(3)				(2385 → 2125)
262.5(2)	30(5)	−0.13(9)		($M1$)	2125 → 1863
271.7(2)	54(7)	0.28(8)	−0.15(9)	($E2$)	
288.8(4)	11(2)				
310.5(2)	60(7)	−0.25(7)	0.03(8)	$E1$ or $M1$	
313.0(3)	18(3)				
317.1(2)	139(13)	−0.22(13)		($M1$)	1863 → 1546
319.8(2)	48(6)				919 → 599
322.0(1)	1000	0.21(6)	−0.11(7)	$E2$	471 → 149
341.7(4)	38(5)				
351.6(3)	21(4)				1303 → 951
355.9(1)	185(15)	0.23(7)	−0.11(8)	$E2$	529 → 173
380.2(1)	156(14)	−0.81(7)	0.15(8)	$M1/E2$	529 → 149
383.7(3)	17(3)	−1.3(4)		$M1/E2$	1303 → 919
390.0(2)	66(8)	−0.17(7)	0.08(8)	($M1$)	919 → 529
392.0(2)	156(14)	−0.19(6)	0.06(7)	($E1$)	1381 → 989
393.4(3)	37(6)	0.45(17)		($E2$)	1939 → 1546
403.8(4)	13(2)				
413.2(4)	20(4)	−0.42(22)	−0.04(24)		
423.5(3)	38(6)				
430.4(2)	181(16)	0.33(6)	0.01(6)	$E1$	1381 → 951
447.8(3)	36(6)				919 → 471
450.2(2)	199(18)	−0.85(8)	0.20(9)	$M1/E2$	599 → 149
453.6(3)	35(6)	0.20(15)	−0.17(17)	($E2$)	1925 → 1471
456.1(3)	20(4)	0.34(12)		($E2$)	2581 → 2125
460.2(1)	186(17)	0.28(8)	−0.06(9)	$E2$	989 → 529
480.0(1)	478(38)	0.26(7)	−0.11(7)	$E2$	951 → 471
482.5(4)	17(3)	−0.86(23)		($M1/E2$)	
518.4(2)	95(11)	−0.85(12)	0.14(14)	$M1/E2$	989 → 471
525.9(3)	37(7)	0.05(12)			
527.3(3)	47(8)	0.27(11)		($E2$)	
542.7(4)	28(6)	−0.24(11)		($E1$ or $M1$)	
559.3(3)	119(20)	0.41(23)		($E2$)	1158 → 599
579.4(2)	110(18)	0.30(8)	−0.09(8)	$E2$	2125 → 1546
591.1(3)	59(11)				1581 → 989
599.3(2)	180(26)				1550 → 951
605.7(3)	39(7)				
612.8(4)	18(4)				
673.1(4)	17(4)	−0.77(33)	0.19(36)	$M1/E2$	
683.0(2)	129(23)	0.19(9)	−0.08(10)	$E2$	2233 → 1550
687.3(2)	180(27)	−0.79(8)	0.25(10)	$M1/E2$	1158 → 471

TABLE I. (*Continued*)

γ-ray energy (keV)	Relative intensity at 125°	Angular distribution A_2/A_0	A_4/A_0	Inferred multipolarity	Placement (keV)
703.3(4)	22(4)				1303 → 599
707.2(3)	38(7)	0.35(14)		(*E*2)	2941 → 2233
709.4(3)	42(7)	0.40(13)		(*E*2)	
831.6(3)	54(8)	−1.14(19)	0.05(21)	*M*1/*E*2	1303 → 471
838.6(4)	23(5)				

[a] Observed only in delayed γ-ray spectra.

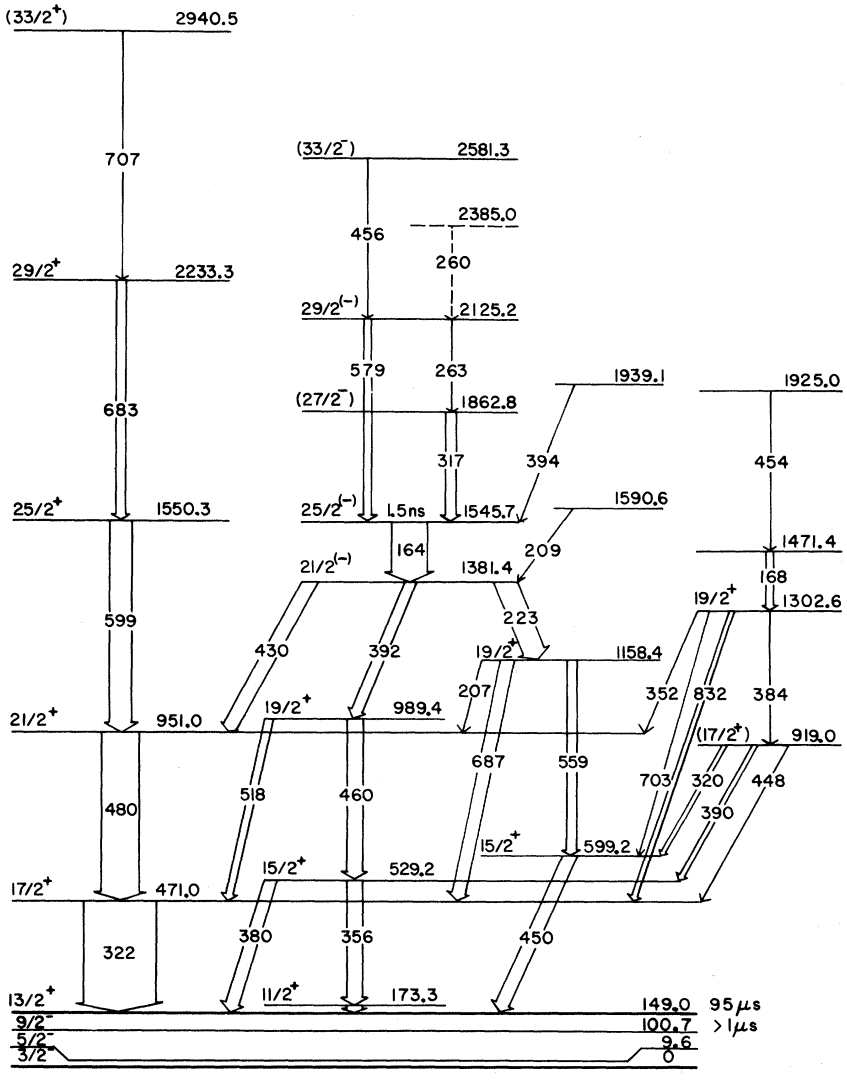

FIG. 4. The ^{191}Pt level scheme. The widths of the transition arrows are proportional to the transition intensities.

TABLE II. Transitions in ^{193}Pt observed in the reaction ^{192}Os(α, 3n) with 35.0 MeV α particles. Estimated uncertainties in the least significant figures are shown in parentheses.

γ-ray energy (keV)	Relative intensity at 125°	Angular distribution A_2/A_0	A_4/A_0	Inferred multipolarity	Placement (keV)
49.2	14(4)				199 → 150
133.9(2)	257(15)	0.33(6)	−0.09(7)	$E2$	1455 → 1321
159.7(3)	19(3)	−0.10(8)			
161.0(2)	96(9)	−0.18(6)	0.02(7)	($E1$)	1321 → 1160
168.8(3)	14(3)	−0.62(16)			
189.5(2)	55(7)	−0.04(6)	0.06(7)		1510 → 1321
216.1(3)	17(3)				
235.2(1)	159(13)	−0.05(6)	0.00(7)	($M1$)	1690 → 1455
255.4(3)	19(4)				
264.1(2)	85(9)	0.35(7)	0.01(8)	($E2$)	
266.5(3)	20(4)	0.57(21)		($E2$)	1777 → 1510
296.8(3)	32(5)				(1987 → 1690)
302.3(2)	23(4)				1992 → 1690
304.0(2)	37(5)	−0.75(11)	0.10(12)	$M1/E2$	907 → 603
317	a				1321 → 1003
320.6(1)	542(38)	0.29(6)	−0.07(7)	$E2$	520 → 199
335.1(2)	23(4)				
340.3(2)	747(75)	−0.16(8)	−0.01(9)	($E1$)	1321 → 981
341.2(2)	1000	0.23(8)	−0.04(9)	$E2$	491 → 150
361.0(3)	41(6)	0.31(7)		($E2$)	2696 → 2335
369.8(1)	150(12)	−0.73(6)	0.08(7)	$M1/E2$	520 → 150
377.3(2)	58(7)	0.31(8)	−0.06(9)	$E2$	981 → 603
387.9(2)	42(6)	−0.36(13)	0.06(15)	($M1/E2$)	907 → 520
413.1(3)	20(4)	0.29(12)			
416.5(2)	50(7)	0.28(9)			907 → 491
425.1(4)	11(2)				
433.0(3)	23(4)				3129 → 2696
447.3(2)	60(7)	0.22(11)			
453.5(1)	238(19)	−0.72(6)	0.09(7)	$M1/E2$	603 → 150
461.0(1)	501(35)	0.30(6)	−0.08(7)	$E2$	981 → 520
474.1(2)	92(9)	−0.07(8)	−0.01(9)		
478.2(3)	26(5)	0.46(23)			
489.5(1)	346(28)	−0.74(8)	0.11(10)	$M1/E2$	981 → 491
500.2(3)	28(5)	−0.44(17)		($M1/E2$)	1104 → 603
503.6(3)	33(6)				
512.4(3)	350(53)				1003 → 491
518.4(4)	16(4)				
537.4(2)	142(17)	0.40(10)	−0.12(11)	$E2$	1992 → 1455
547.2(3)	31(6)	−1.03(33)		($M1/E2$)	
556.5(3)	77(10)	0.23(13)	−0.03(15)	($E2$)	1160 → 603
595.7(3)	49(8)	0.53(22)			
628.4(2)	228(23)	0.36(7)	−0.11(8)	$E2$	1632 → 1003
640.2(4)	34(7)	0.33(17)		($E2$)	1160 → 520
669.1(3)	117(17)	−0.60(9)	0.19(11)	$M1/E2$	1160 → 491
703.4(3)	121(18)	0.40(8)	−0.13(10)	$E2$	2335 → 1632

[a]Obscured by intense 316.5 keV ^{192}Pt γ rays.

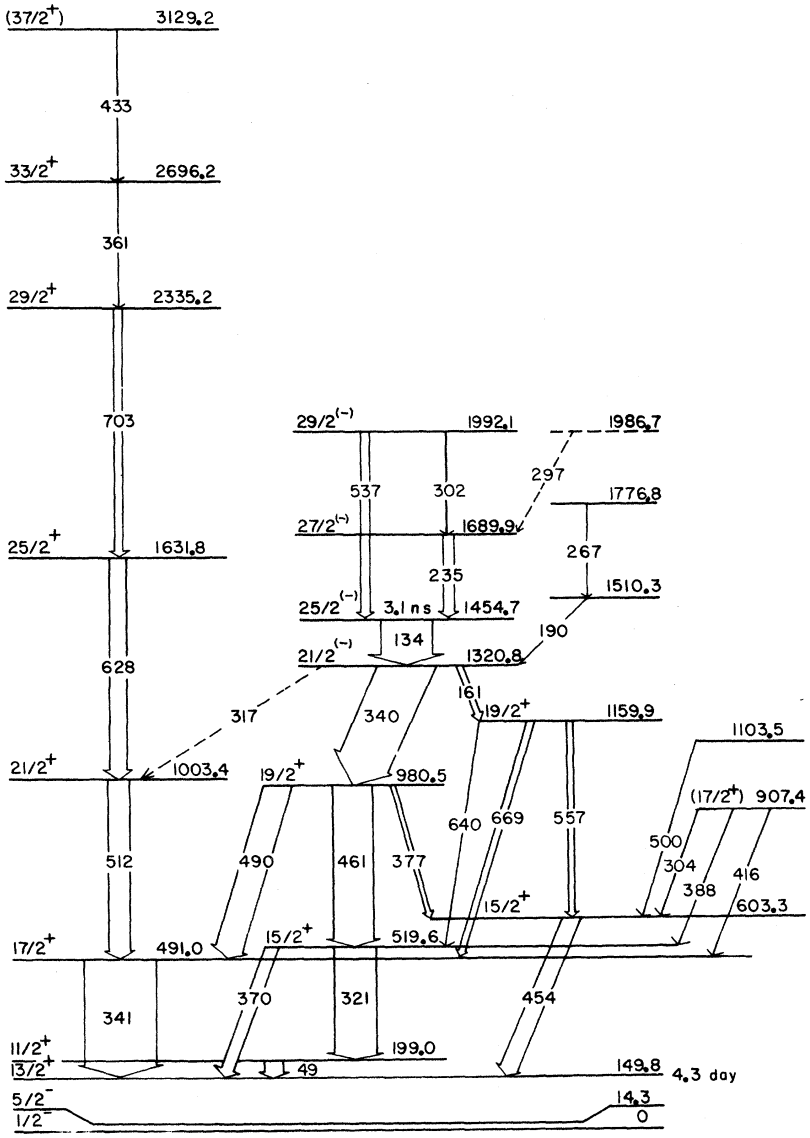

FIG. 5. The ^{193}Pt level scheme. The widths of the transition arrows are proportional to the transition intensities.

been, of course, a familiar problem, encountered in earlier triaxial rotor calculations,[1,2] and attributed to the known softness of the even-even core. As Toki and Faessler have shown,[2] it can be handled by an extended VMI treatment. The other discrepancy was that the distinctly different de-excitation properties of the two low-lying $\frac{15}{2}^+$ levels were not reproduced in the calculation. Since the calculated energy separation of these two levels was only 29 keV compared to 70 keV experimentally, it was conjectured[5] that an overestimate of the mixing between the two $\frac{15}{2}^+$ states may have been responsible for the incorrect branching ratios.

More recently we have performed additional calculations in which the deformation parameter β was adjusted until the energies of the $\frac{17}{2}^+$ and $\frac{21}{2}^+$ members of the favored decoupled band were reproduced closely. In both cases, an increase of 5–10% over the values of β derived from the 2^+-0^+ spacings in the adjacent even-even nuclei was sufficient. This change, which may be regarded as a first-order compensation for the known increase in the effective moment of inertia of a soft nucleus at higher angular momentum, had the effect of lowering all the calculated energies. The lowering was most pronounced for the unfavored

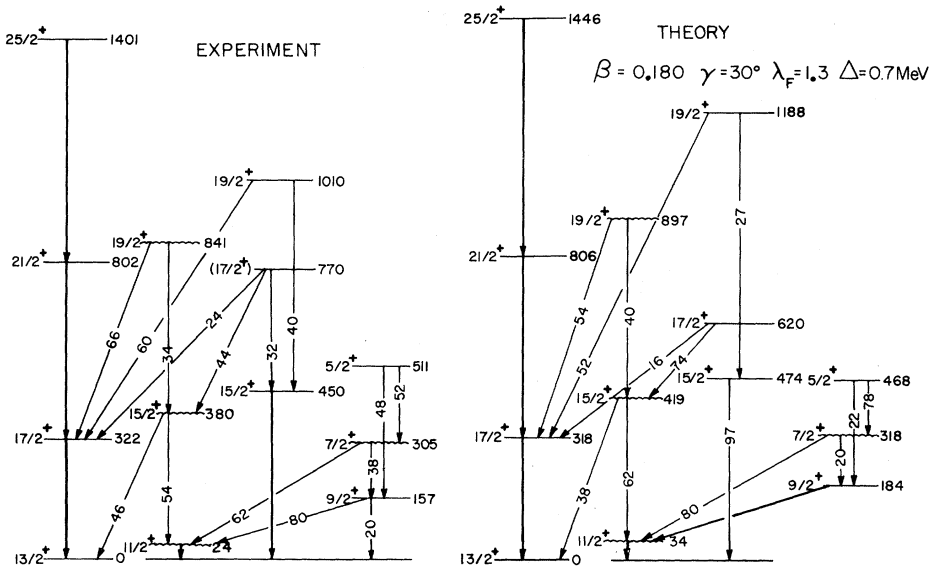

FIG. 6. A comparison of experimental and theoretical energies and branching ratios of positive parity levels in ^{191}Pt. The energies are expressed relative to zero energy for the $\frac{13}{2}^+$ level, and the parameters β, γ, λ_F, and Δ are those defined in Ref. 1. Relative branching intensities are shown as percentages, except for transitions with branching intensities less than 15%, which are omitted from this comparison. The theoretical intensities were determined using calculated $B(M1)$ and $B(E2)$ values, but experimental energies. The members of the unfavored $(j-1)$ band are shown as wavy lines.

levels, in line with the expectation that an increase in deformation will tend to favor strong coupling. The modest increase in β resulted in decidedly better agreement with the experimental energies and branching intensities, as is illustrated in Fig. 6 for the ^{191}Pt nucleus. In particular, the calculated separation of the two $\frac{15}{2}^+$ levels is now much closer to that observed and their distinctive branching patterns are accurately reproduced. It is emphasized that the calculations reproduced the energies and branching ratios of the positive parity levels in ^{193}Pt equally well; the comparison for the ^{191}Pt nucleus has again been chosen for illustration here only because the low-spin as well as the high-spin ^{191}Pt levels are known.

One of the more interesting aspects of the present study has been the location of very low-lying $(j-1)$ unfavored bands of $\nu i_{13/2}$ levels in each of the odd-A Pt nuclei, and the success of the triaxial rotor model in describing them. The $\frac{11}{2}^+$ bandhead lies 49 and 24 keV above the $\frac{13}{2}^+$ level in ^{193}Pt and ^{191}Pt, respectively, and in ^{189}Pt the corresponding $\frac{11}{2}^+$ level has been found[14] only 11 keV above the $\frac{13}{2}^+$ level. Two factors can be expected to contribute towards the lowering of the energies of the unfavored levels as the mass number decreases. One is the location of the Fermi surface deeper within the $\nu i_{13/2}$ shell. The other is the decrease of γ below 30°, approaching a prolate shape and therefore favoring strong coupling over decoupling. Presumably, as the core becomes more prolate, the $\frac{11}{2}^+$ level will be found at still lower energies in lighter odd-A Pt nuclei, until a strong-coupled level ordering, such as is seen in odd-A Os nuclei, is attained.

V. CONCLUSION

The present investigation has shown that the triaxial rotor plus hole model, which has previously been successful in describing families of $\pi h_{11/2}$ and $\pi h_{9/2}$ levels in the $A \sim 190$ region, can equally well account for extensive new experimental data for $\nu i_{13/2}$ level families in ^{191}Pt and ^{193}Pt. The experiments show, and the model calculations accurately reproduce, characteristic low-lying $(j-1)$ unfavored bands, which are a consequence of the location of the Fermi surface within the $\nu i_{13/2}$ subshell. These results tend to support the proposal that $A \sim 190$ nuclei have rather stable triaxial shapes.

We thank J. Meyer ter Vehn for many fruitful discussions and for providing us with a copy of his program.

*Research supported by the U. S. Energy Research and Development Administration and the National Science Foundation.

†Present address: Physics Department, University of Jyväskylä, Finland.

‡Present address: Babcock and Wilcox, Lynchburg, Virginia.

[1]J. Meyer ter Vehn, Nucl. Phys. A249, 111, 141(1975).

[2]H. Toki and A. Faessler, Z. Phys. A276, 35 (1976).

[3]M. Piiparinen, J. C. Cunnane, P. J. Daly, C. L. Dors, F. M. Bernthal, and T. L. Khoo, Phys. Rev. Lett. 34, 1110 (1975).

[4]M. Piiparinen, S. K. Saha, P. J. Daly, T. L. Khoo, C. L. Dors, and F. M. Bernthal, Nucl. Phys. A265, 253 (1976).

[5]T. L. Khoo, F. M. Bernthal, C. L. Dors, M. Piiparinen, S. K. Saha, P. J. Daly, and J. Meyer ter Vehn, Phys. Lett. 60B, 341 (1976).

[6]J. C. Cunnane, M. Piiparinen, P. J. Daly, C. L. Dors, T. L. Khoo, and F. M. Bernthal, Phys. Rev. C 13, 2197 (1976).

[7]M. Piiparinen, S. K. Saha, P. J. Daly, C. L. Dors, F. M. Bernthal, and T. L. Khoo, Phys. Rev. C 13, 2208 (1976).

[8]M. B. Lewis, Nucl. Data B 8, 389 (1972).

[9]D. Proetel, D. Benson, Jr., A. Gizon, J. Gizon, M. R. Maier, R. M. Diamond, and F. S. Stephens, Nucl. Phys. A226, 237 (1974); D. Proetel, R. M. Diamond, and F. S. Stephens, *ibid.* A231, 301 (1974).

[10]H. Beuscher, W. F. Davidson, R. M. Lieder, A. Neskakis, and C. Mayer-Böricke, Phys. Rev. Lett. 32, 843 (1974).

[11]K. Neergard, P. Vogel, and M. Radomski, Nucl. Phys. A238, 199 (1975).

[12]S. E. Larsson, Phys. Scr. 8, 17 (1973).

[13]F. S. Stephens and R. S. Simon, Nucl. Phys. A182, 257 (1972).

[14]S. K. Saha *et al.* (unpublished).